NASA/TM—2006-214034

Feasibility Study of Jupiter Icy Moons Orbiter Permanent Magnet Alternator Start Sequence

Barbara H. Kenny
Glenn Research Center, Cleveland, Ohio

Roger P. Tokars
Purdue University, West Lafayette, Indiana

February 2006

The NASA STI Program Office . . . in Profile

Since its founding, NASA has been dedicated to the advancement of aeronautics and space science. The NASA Scientific and Technical Information (STI) Program Office plays a key part in helping NASA maintain this important role.

The NASA STI Program Office is operated by Langley Research Center, the Lead Center for NASA's scientific and technical information. The NASA STI Program Office provides access to the NASA STI Database, the largest collection of aeronautical and space science STI in the world. The Program Office is also NASA's institutional mechanism for disseminating the results of its research and development activities. These results are published by NASA in the NASA STI Report Series, which includes the following report types:

- TECHNICAL PUBLICATION. Reports of completed research or a major significant phase of research that present the results of NASA programs and include extensive data or theoretical analysis. Includes compilations of significant scientific and technical data and information deemed to be of continuing reference value. NASA's counterpart of peer-reviewed formal professional papers but has less stringent limitations on manuscript length and extent of graphic presentations.

- TECHNICAL MEMORANDUM. Scientific and technical findings that are preliminary or of specialized interest, e.g., quick release reports, working papers, and bibliographies that contain minimal annotation. Does not contain extensive analysis.

- CONTRACTOR REPORT. Scientific and technical findings by NASA-sponsored contractors and grantees.

- CONFERENCE PUBLICATION. Collected papers from scientific and technical conferences, symposia, seminars, or other meetings sponsored or cosponsored by NASA.

- SPECIAL PUBLICATION. Scientific, technical, or historical information from NASA programs, projects, and missions, often concerned with subjects having substantial public interest.

- TECHNICAL TRANSLATION. English-language translations of foreign scientific and technical material pertinent to NASA's mission.

Specialized services that complement the STI Program Office's diverse offerings include creating custom thesauri, building customized databases, organizing and publishing research results . . . even providing videos.

For more information about the NASA STI Program Office, see the following:

- Access the NASA STI Program Home Page at ***http://www.sti.nasa.gov***

- E-mail your question via the Internet to help@sti.nasa.gov

- Fax your question to the NASA Access Help Desk at 301–621–0134

- Telephone the NASA Access Help Desk at 301–621–0390

- Write to:
  NASA Access Help Desk
  NASA Center for AeroSpace Information
  7121 Standard Drive
  Hanover, MD 21076

NASA/TM—2006-214034

Feasibility Study of Jupiter Icy Moons Orbiter Permanent Magnet Alternator Start Sequence

Barbara H. Kenny
Glenn Research Center, Cleveland, Ohio

Roger P. Tokars
Purdue University, West Lafayette, Indiana

National Aeronautics and
Space Administration

Glenn Research Center

February 2006

Available from

NASA Center for Aerospace Information
7121 Standard Drive
Hanover, MD 21076

National Technical Information Service
5285 Port Royal Road
Springfield, VA 22100

Available electronically at http://gltrs.grc.nasa.gov

Feasibility Study of Jupiter Icy Moons Orbiter Permanent Magnet Alternator Start Sequence

Barbara H. Kenny
National Aeronautics and Space Administration
Glenn Research Center
Cleveland, Ohio 44135

Roger P. Tokars
Purdue University
Electrical and Computer Engineering Department
West Lafayette, Indiana 47906

Abstract

The Jupiter Icy Moons Orbiter (JIMO) mission was a proposed, (recently cancelled) long duration science mission to study three moons of Jupiter: Callisto, Ganymede, and Europa. One design of the JIMO spacecraft used a nuclear heat source in conjunction with a Brayton rotating machine to generate electrical power for the electric thrusters and the spacecraft bus. The basic operation of the closed cycle Brayton system was as follows. The working fluid, a helium-xenon gas mixture, first entered a compressor, then went through a recuperator and hot-side heat exchanger, then expanded across a turbine that drove an alternator, then entered the cold-side of the recuperator and heat exchanger and finally returned to the compressor. The spacecraft was to be launched with the Brayton system off-line and the nuclear reactor shut down. Once the system was started, the helium-xenon gas would be circulated into the heat exchangers as the nuclear reactors were activated. Initially, the alternator unit would operate as a motor so as to drive the turbine and compressor to get the cycle started. This report investigated the feasibility of the start up sequence of a permanent magnet (PM) machine, similar in operation to the alternator unit, without any position or speed feedback sensors ("sensorless") and with a variable load torque. It is found that the permanent magnet machine can start with sensorless control and a load torque of up to 30 percent of the rated value.

Introduction

In addition to the interesting science objectives, the proposed JIMO mission would also have been an opportunity to demonstrate several technologies in the harsh environment of space. A nuclear fission reactor was to provide the heat source for a dynamic power conversion cycle that ultimately produced electricity for the spacecraft use. The propulsion system was based on electric thrusters. The spacecraft electrical power system was approximately two orders of magnitude larger than anything previously flown. The entire spacecraft needed to operate reliably and semi-autonomously for over a decade with part of the time in the radiation environment of Jupiter.

One option for the proposed JIMO power system was based on a Brayton cycle with a helium-xenon gas mixture as the working fluid. The block diagram of the cycle is shown in figure 1. In this option, once at steady state, the alternator is regulated using a parasitic shunt resistor as described in reference 1. This keeps the speed of the machine (and therefore the bus voltage) approximately constant regardless of load.

At start-up, however, there is not enough energy in the working fluid to turn the turbine and compressor. This must be accomplished by a motoring action, either through an additional machine attached to the shaft and only used at start-up, or by operating the alternator as a motor during the start-up transition. A permanent magnet machine is the most likely candidate for the alternator and it can operate as either a motor or generator depending on how it is controlled. For optimal operation as a motor, the controller requires rotor position information so that the applied voltage and current can be oriented

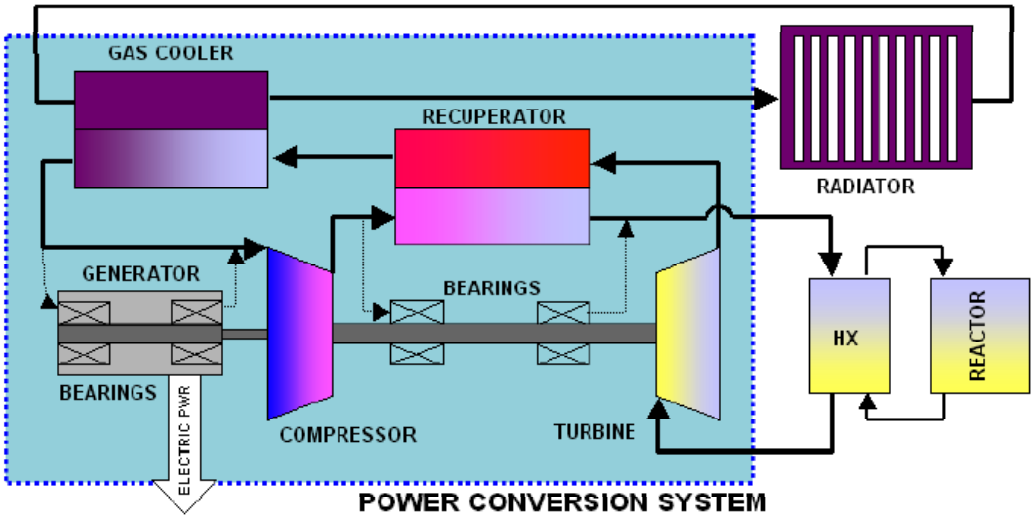

Figure 1.—Representative block diagram of Brayton cycle (actual design may differ), HX = heat exchanger, "generator" block represents alternator function.

properly with respect to the rotor field. Typically this is done using either Hall Effect sensors, a resolver or an encoder. However, these sensors add complexity and failure modes to the system and they may be sensitive to radiation and thus not perform properly in the Jupiter environment. Hence this investigation was undertaken to see if the PM machine could be reliably started and operated as a motor without any rotor position or magnetic field feedback sensors.

There are many papers in the literature about sensorless operation of PM machines (refs. 2, 3, 4, and 5) and mid- to high-speed operation is fairly straight-forward. The difficulty comes at low- and zero-speeds, especially with significant load torques that require large machine currents. One technique involves adding an additional voltage signal to the fundamental voltage but requires that the machine rotor have a magnetic saliency (inductance variation with rotor position) (refs. 6 and 7). This technique may have been a viable candidate to start the JIMO machine because the alternator could have been designed and built with a suitable saliency. However, as a baseline case, it was desired to determine if a PM machine could be started under load without any additional sensing signal and/or special design.

In this work, the machine was started from zero speed up to a few hundred rpm without any knowledge of the position of the rotor field. In this sense it was an "open loop" start although current magnitude was measured and regulated. Then the control was transitioned to a technique known as field orientation control or vector control (refs. 8, 9, 10, and 11) where a rotor position estimate, in addition to the current magnitude command, was used to determine the commanded voltage to the machine. After establishing the field orientation control, a loop was then closed on speed to regulate the rate of start-up.

Nomenclature

L_q is the q-axis machine inductance, henries.

L_d is the d-axis machine inductance, henries.

f^x_{qy} represents a q-axis scalar quantity where f can be voltage, v, current, i, or flux, λ; x can be the rotor reference frame, r, or the stator reference frame, s; and y is either the stator variable, s, or the rotor variable, r.

f^x_{dy} represents a d-axis scalar quantity where f can be voltage, v, current, I, or flux, l; x can be the rotor reference frame, r, or the stator reference frame, s; and y is either the stator variable, s, or the rotor variable, r.

$\mathbf{f}^{x}_{qdy}$ represents the d-q vector quantity where f can be voltage, v, current, I, or flux, λ; x can be the rotor reference frame, r, or the stator reference frame, s; and y is either the stator variable, s, or the rotor variable, r.

* a superscript asterisk represents a commanded value.

$\wedge$ a carrot above a symbol represents an estimated quantity.

p is the derivative operator, d/dt.

θ_r is the angle between the stator q-axis and the rotor q-axis, radians.

λ_{af} is the flux linkage due to the rotor magnets, volt-sec.

ω_r is the electrical rotor speed, radians/second.

P is the number of poles of the machine.

Field Orientation Control

The basic idea behind field orientation control is to orient the applied stator currents to the rotor magnetic field. When this is done, the motor control is simplified because the control variables become dc quantities in steady state. The operating point of the machine can then be accurately and dynamically controlled so that high efficiency and fast response are obtained. Accurate torque, speed or position control of the machine is then possible depending on the outer loop used. A detailed discussion can be found in many electric machine textbooks (refs. 8, 9, 10, and 11).

The key to successful field orientation control is accurate and continuous knowledge of the position of the rotor magnetic field. Typically this is done with a position sensor (resolver or encoder) or a magnetic field sensor (Hall Effect). In "sensorless" control, this sensor is eliminated and the position of the rotor field is estimated using measured machine currents. This section describes basic field orientation control, the next section explains the open loop starting procedure without knowledge of the rotor position, and the following section describes the technique used to estimate the rotor position.

A three phase machine, without a neutral connection, can be equivalently described as a two phase machine through a transformation from abc coordinates to dq coordinates as follows:

$$f_q = f_a \tag{1}$$

$$f_d = -\frac{1}{\sqrt{3}} f_a - \frac{2}{\sqrt{3}} f_b \tag{2}$$

The reverse transformation is

$$f_a = f_q \tag{3}$$

$$f_b = -\frac{1}{2} f_q - \frac{\sqrt{3}}{2} f_d \tag{4}$$

$$f_c = -\frac{1}{2} f_q + \frac{\sqrt{3}}{2} f_d \tag{5}$$

The d and q variables described in equations (1) and (2) are in the stator reference frame. From equation (1) it can be seen that the q-axis is aligned with the 'a' phase. This means that the 'a' phase current is equal to the q-axis current and the 'a' phase voltage (V_{an}) is equal to the q-axis voltage.

In a permanent magnetic machine, it is convenient to transform these variables to a reference frame that is rotating synchronously with the rotor magnetic field. In the rotor reference frame, the d-axis is defined to be co-linear with the rotor magnetic field axis. The transformation from the stator frame to the rotor frame is given by equation (6) and the inverse transformation is given by equation (7).

$$\begin{bmatrix} f_q^r \\ f_q^r \end{bmatrix} = \begin{bmatrix} \cos\theta_r & -\sin\theta_r \\ \sin\theta_r & \cos\theta_r \end{bmatrix} \begin{bmatrix} f_q^s \\ f_d^s \end{bmatrix} \tag{6}$$

$$\begin{bmatrix} f_q^s \\ f_d^s \end{bmatrix} = \begin{bmatrix} \cos\theta_r & -\sin\theta_r \\ -\sin\theta_r & \cos\theta_r \end{bmatrix} \begin{bmatrix} f_q^r \\ f_d^r \end{bmatrix} \tag{7}$$

The permanent magnetic synchronous machine can then be modeled in the rotor reference frame as follows. Equation (8) gives the voltage relationships in the rotor reference frame, equation (9) gives the stator flux linkages in the rotor reference frame and equation (10) is the torque expression.

$$\begin{bmatrix} V_{qs}^r \\ V_{ds}^r \end{bmatrix} = \begin{bmatrix} R_s + L_q p & \omega_r L_d \\ -\omega_r L_q & R_s + L_d p \end{bmatrix} \begin{bmatrix} i_{qs}^r \\ i_{ds}^r \end{bmatrix} + \begin{bmatrix} \omega_r \lambda_{af} \\ 0 \end{bmatrix} \tag{8}$$

$$\begin{bmatrix} \lambda_{qs}^r \\ \lambda_{ds}^r \end{bmatrix} = \begin{bmatrix} Lq & 0 \\ 0 & L_d \end{bmatrix} \begin{bmatrix} i_{qs}^r \\ i_{ds}^r \end{bmatrix} + \begin{bmatrix} 0 \\ \lambda_{af} \end{bmatrix} \tag{9}$$

$$T_e = \frac{3P}{4} \left[\lambda_{ds}^r \, i_{qs}^r - \lambda_{qs}^r \, i_{ds}^r \right] \tag{10}$$

In field orientation control the d-axis current, i_{ds}^r, is commanded to 0. From (9) and (10) it can be seen that this results in a simplified expression for torque, given in (11).

$$T_e = \frac{3P}{4} \left[\lambda_{af} \, i_{qs}^r \right] \tag{11}$$

Because the magnitude of λ_{af} is constant due to the rotor magnets, the torque of the machine is proportional to the q-axis current. This result is similar to the dc motor with a constant field winding current where the torque is equal to the armature current times the torque constant. Thus control of the torque is achieved in the permanent magnet machine by properly controlling the rotor reference frame currents, i_{qs}^r and i_{ds}^r.

To control the currents in the machine to be the commanded values, a current regulated voltage source inverter is used. This means that current errors result in voltage commands to the inverter that increase or decrease the applied voltage to increase or decrease the current, respectively. This is accomplished through a synchronous frame current regulator (ref. 12) that is basically a PI (proportional-integral) controller operating on the rotor reference frame currents. The output of the controller is a voltage command in the rotor reference frame that is then transformed to the stator reference frame. The stator frame voltage commands are then used to calculate the inverter switch duty cycles.

There are several methods to find the duty cycles from the commanded stator frame voltages (ref. 13). In the implementation used here, space vector modulation is used. Space vector modulation is a digital technique to calculate the duty cycles directly from the stator reference frame d and q voltages. One advantage of space vector modulation is that it increases the dc bus utilization to the maximum value. This means that for a given dc bus voltage, the maximum fundamental phase voltage (with minimum low order harmonics) is achievable by using space vector modulation.

Figure 2 shows the overall block diagram of the control structure. As can be seen from equations (6) and (7), rotor position is necessary to perform the field orientation transformation. For zero and low speed operation, the transformation angle is based on a ramped frequency command. After a few hundred rpm, the transformation angle is based on the estimated angle from the estimation algorithm.

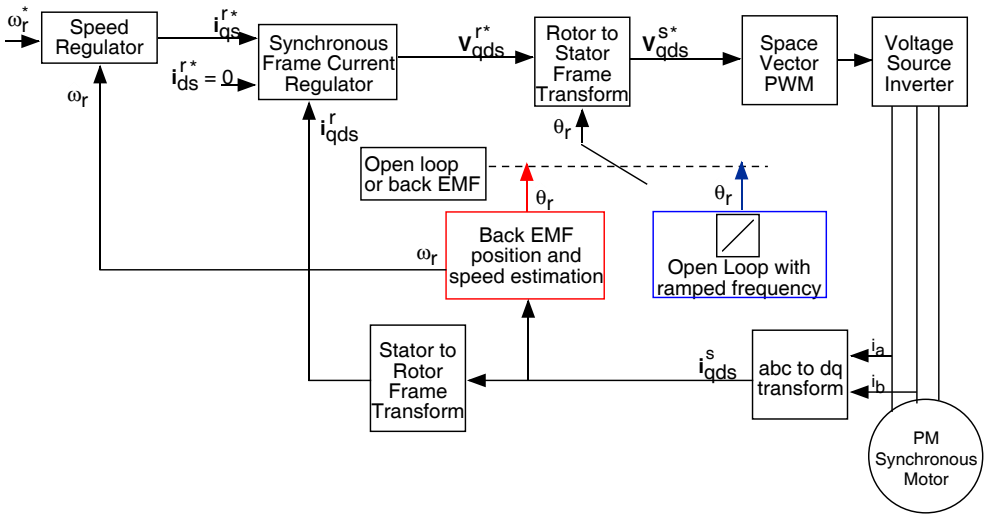

Figure 2.—Basic block diagram of motor control.

Open Loop Starting

The principle behind open loop starting is that a slowly rotating magnetic field can be set up in the air gap of the machine that the rotor magnets will try to follow. As the speed of the magnetic field increases, the rotor speed also increases as it tries to "keep up" with the field. The field must be strong enough to pull the rotor along as the frequency increases. The magnitude of the field is related to the magnitude of the current in the stator windings. A larger inertia rotor will require more current to accelerate than a smaller inertia one. Also, a larger load torque or bearing drag will require more current than a smaller one.

The position of the field is related to the transformation angle, θ_r. The speed of the field is governed by the rate of change of the transformation angle, $\frac{d\theta_r}{dt}$. The acceleration rate is the second derivative of the transformation angle, $\frac{d^2\theta_r}{dt^2}$. During the open loop portion of the control, the acceleration rate is governed by the ramp rate as shown in the block diagram of figure 2. In open loop starting, the current magnitude and the acceleration rate of the rotating field are the command variables. Although they must work together to keep the rotor accelerating, there is not a one-to-one correspondence between them. For example, there is a range of acceleration rates that would work with a particular current command and a range of current commands that would work with a particular acceleration rate. The slack variable is the efficiency of the motor operation that is not controlled during open loop starting. However, the current and acceleration rate commands must be set with some general knowledge of the inertia and the load torque of the system.

The predominant load torque for starting the JIMO alternator was expected to be the bearing drag. One Brayton shaft design used foil bearings to minimize bearing wear during the long mission (ref. 14). Foil bearings are very low loss beyond some minimal speed, however at low speed and zero speeds; there is direct contact between the shaft and the bearing raceway. This contact generates heat as the shaft turns that can damage the bearings if the minimal "lift off" speed is not attained quickly. The problem for the open loop portion of the motor control is that an exact bearing drag torque model for foil bearings has not been developed. The drag torque depends on several factors as the rotor accelerates. Some of what is known is based on empirical data from testing foil bearings and additional tests would have been conducted on the final JIMO machine design but at the time of this work, there was no exact model of the foil bearing drag torque during start-up conditions. So the open loop motor control needed to be robust enough to start the machine even though the exact drag torque could not yet be predicted. However, once

the machine control changed to field orientation, the rotor speed could be controlled to the commanded value regardless of the drag torque or any other load torque.

Position Estimate

The rotor position (and speed) estimate is based on a technique known as back EMF (electro-motive force) estimation. The "back EMF" technique derives its name from the fact that the spinning rotor magnets will generate a voltage (the back EMF) at the terminals of the machine. This voltage can be integrated to find the stator flux (ref. 4). From the stator flux vector and an estimate of the torque angle, the rotor flux position can be estimated (ref. 3). This will be described next.

The stator reference frame equation describing the relationship between the stator voltage, current and flux linkages for the fundamental excitation of the machine is given in equation (12).

$$\mathbf{v}^{s}_{qds} = \mathbf{i}^{s}_{qds}\mathbf{R}_{s} + p\boldsymbol{\lambda}^{s}_{qds} \tag{12}$$

The stator flux can be estimated by integrating the stator voltage less the IR drop as shown in equation (13).

$$\boldsymbol{\lambda}^{s}_{qds} = \int \left(\mathbf{v}^{s}_{qds} - \mathbf{i}^{s}_{qds}\mathbf{R}_{s}\right) dt \tag{13}$$

In the simplest implementation (used in this work), the stator voltage, $\mathbf{v}^{s}_{qds}$, is assumed to be equal to $\mathbf{v}^{s*}_{qds}$, the commanded voltage, which is known in the controller. This is equivalent to assuming a constant dc bus voltage and no voltage loss in the inverter. Improvements in the flux estimate by using either better estimates of stator voltage or by actually measuring stator voltage are possible and described in the literature.

Additionally, the open loop integration described by equation (13) was actually implemented as a low pass filter with a 25 Hz bandwidth. This low pass filter implementation requires an adjustment of the estimated angle at very low speeds (below about 1500 rpm) due to the phase shifting properties of the low pass filter. However, this is easily accomplished with a look-up table. The technique was found experimentally to result in a reliable rotor position estimate at speeds above about 300 rpm.

The stator flux vector can be found from equation (13) but it is knowledge of the position of the rotor flux, λ_{af}, which is necessary for proper field orientation. This can be found by expressing the stator flux in the rotor reference frame wherein the d-axis component of the stator flux vector is aligned with the rotor flux, λ_{af}.

$$\lambda^{r}_{qs} = L_{q} i^{r}_{qs} \tag{14}$$

$$\lambda^{r}_{ds} = L_{d} i^{r}_{ds} + \lambda_{af} \tag{15}$$

The angle between the stator flux vector, $\boldsymbol{\lambda}_{qds}$, and λ_{af} is the torque angle which is found from equations (14) and (15).

$$\delta = \tan^{-1}\left(\frac{\mathbf{L}_{q}\mathbf{i}^{r}_{qs}}{\mathbf{L}_{d}\mathbf{i}^{r}_{ds} + \boldsymbol{\lambda}_{af}}\right) \tag{16}$$

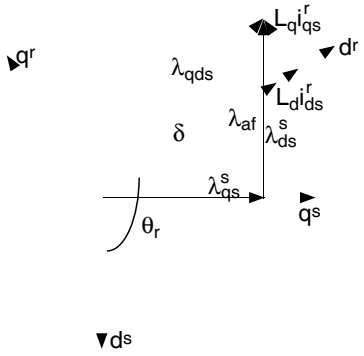

Figure 3.—Vector diagram showing flux, current, angles, and reference frame axes.

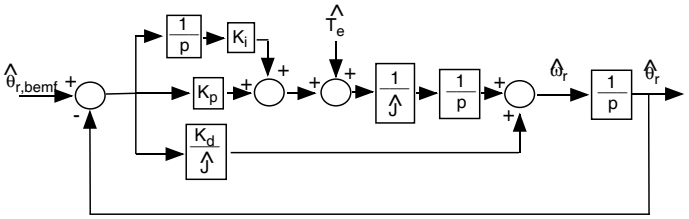

Figure 4.—Speed observer.

These relationships can be best shown graphically as in figure 3. For field orientation control, the d-axis of the rotor reference frame is defined to be coincident with the rotor flux. To transform from the stator frame to the rotor reference frame, the rotor angle, θ_r, must be known. This is the angle between the stator frame d-axis and the rotor frame d- axis (or, equivalently, the angle between the stator frame q-axis and the rotor frame q-axis) as shown in figure 3. Mathematically, this angle can be found from equation (17) as shown.

$$\hat{\theta}_r = \tan^{-1}\left(\frac{\lambda^s_{qs}}{\lambda^s_{ds}}\right) - \delta \tag{17}$$

The estimated rotor angle, $\hat{\theta}_r$, is used for the reference frame transformations as shown in figure 2 and is also used as an input into a speed observer as shown in figure 4. A torque estimate can also be used to improve the response of the speed estimate reference 15.

At 300 rpm, the position estimate is accurate enough to use as the transformation angle shown in figure 2. At this point the open loop control can be discontinued and field orientation control can be used reliably. Once under field orientation, the acceleration of the machine is completely controlled by the commanded current value. The speed loop is closed next (using the estimate shown in figure 4 as feedback) and then the current command becomes the result of the speed loop error rather than being commanded explicitly.

Simulation Results

The simulation used a model of a representative permanent magnet machine based on the expected power requirements of the alternator. The assumed parameters are given in table 1. The control consisted of a closed loop current regulator, the open loop starting sequence, field orientation control, and the rotor position/speed estimation algorithm described in the previous section. The start-up bearing drag torque was modeled as a linear function that decreased with speed to a small constant value at 4500 rpm. That function is given in equations (18) and (19). The simulation was written in Matlab/Simulink. The results are presented in figures 5 to 8.

$$T_L \text{ (N-m)} = 7.0 - 0.0015 * \text{speed (rpm)} \qquad \text{for } 0 \le \text{speed} < 4500 \text{ rpm} \tag{18}$$

$$T_L \text{ (N-m)} = 0.2 \qquad \text{for speed} \ge 4500 \text{ rpm} \tag{19}$$

TABLE 1.—MACHINE PARAMETERS USED IN SIMULATIONS

Machine Parameter	Value
J	0.01 kg-m^2
L_s	34 μH
R_s	0.03 Ω
λ_{af}	0.023 volt-sec
Poles	6
Rated torque	21 N-m
Rated current	144 amps (rms)

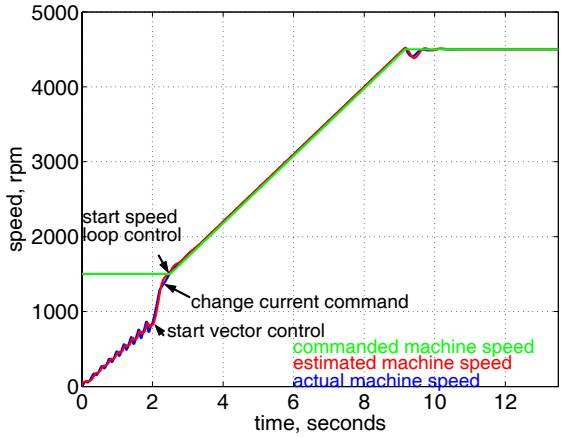

Figure 5.—Machine speed during start-up: actual, estimated, and commanded.

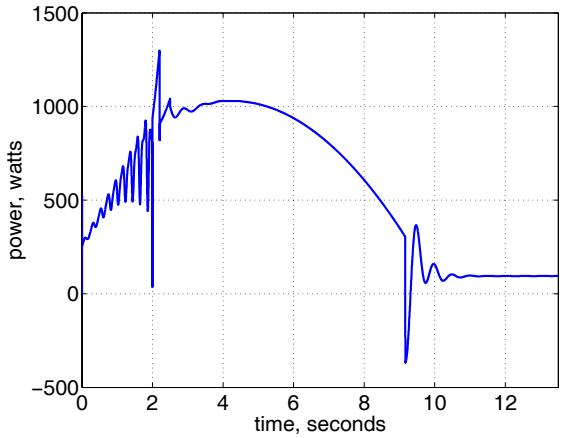

Figure 6.—Machine power during start up.

The simulation begins with an acceleration ramp rate of 400 rpm/second and a current magnitude command of 75 amps (peak). At t = 2 seconds (machine at ~850 rpm) the control switches from open loop to field orientation. At t = 2.2 seconds, the current command is reduced to 55 amps and at t = 2.5 seconds the speed loop is closed. Acceleration continues based on a ramped speed command of 400 rpm/second until the commanded value of 4500 rpm is reached at t = 9 seconds.

Figure 5 shows the commanded speed, the estimated speed and the actual speed of the machine. The estimated speed can be seen to agree with the actual speed very closely although the actual speed demonstrates some ringing during the open loop portion of the control. If the control is not switched over to field orientation in time, the machine will reach a speed where this ringing becomes large enough to

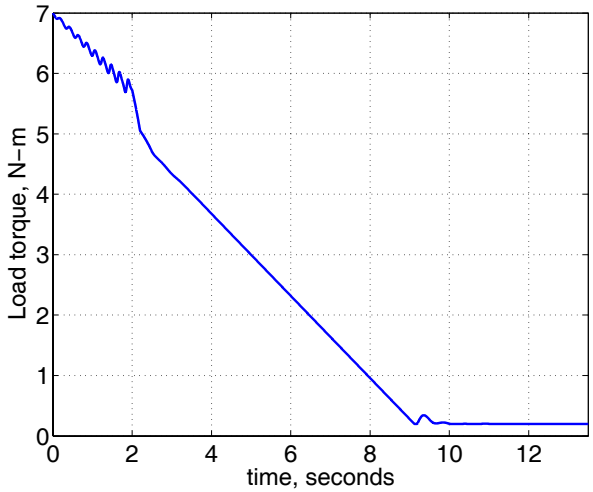

Figure 7.—Load torque characteristics.

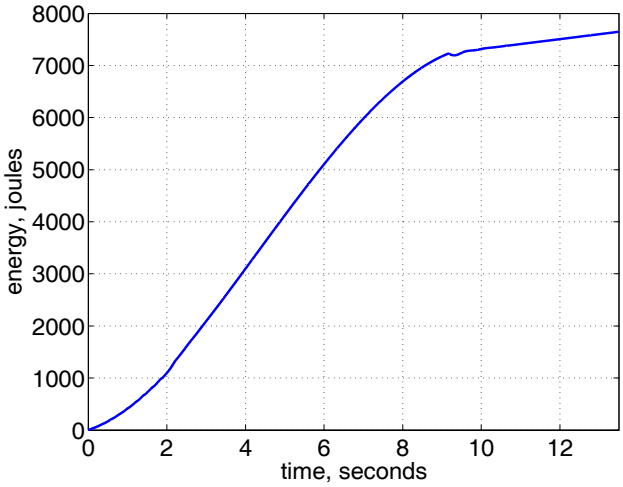

Figure 8.—Energy required to start machine.

cause the machine to cease accelerating and to lose synchronism; the starting procedure fails. Also, it appeared during the simulation trials that lower speeds were more tolerant of variations in the ramp rate and the commanded current level than higher speeds. So for an actual implementation, it would be important to switch over to field orientation control as soon as practical to guarantee good performance.

Figures 6 and 7 also show ringing during the open loop start portion of the control and this is because the actual machine speed was used in the simulation to calculate the load torque (eq. (18)) and the machine power, respectively.

Experimental Set-Up

The experimental set-up consisted of a 4 pole PM machine, a Magtrol hysteresis dynamometer, an 1103 dSpace Controller and a Semikron IGBT inverter switching at 20 kHz. The PM machine was designed in a "back-to-back" configuration—there are two stators and two rotor pieces mounted on the same shaft with a small steel flywheel in between. The machine has an inertia of approximately 4.654 e-4 kg-m^2. The dynamometer has an inertia of 1.49 e-3 kg-m^2. A picture of the set up is shown in figure 9 and the machine parameters are given in table 2. Only one stator of the PM machine was connected to the output of the Semikron inverter and the other stator was left open. The machine is rated for 60,000 rpm operation and the peak power at full speed is 9 kw.

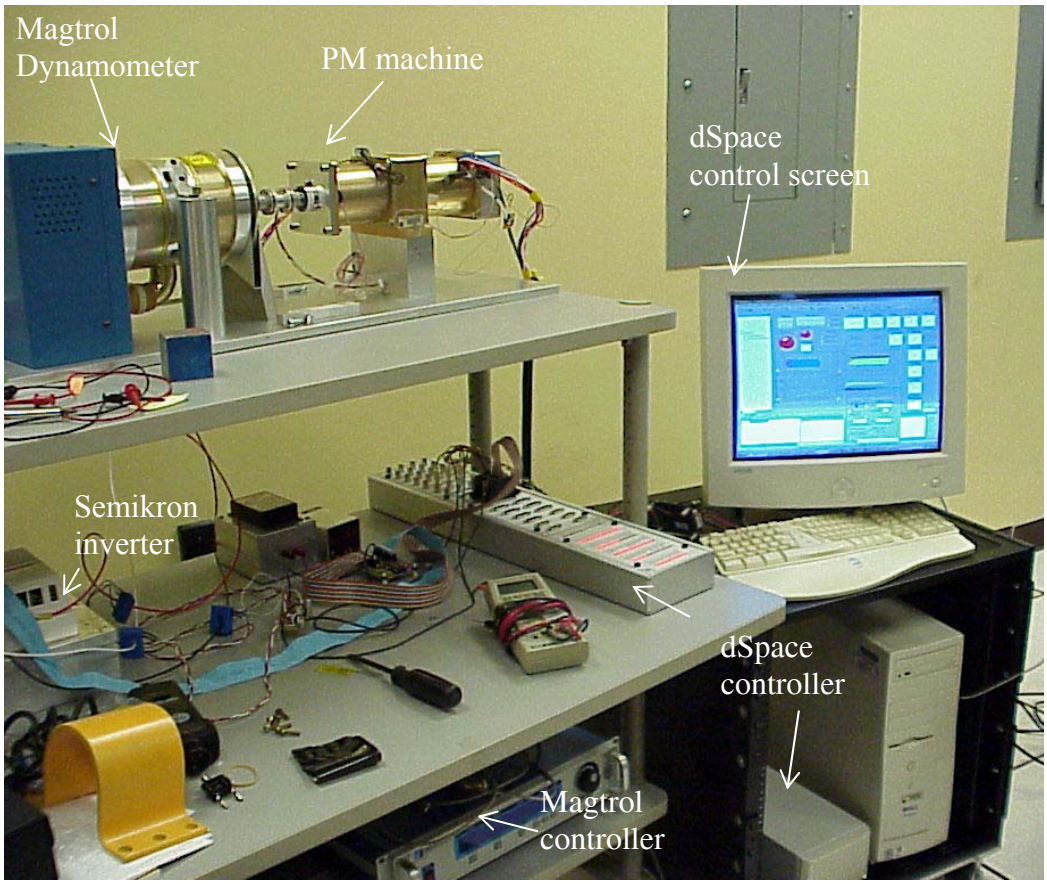

Figure 9.—Experimental demonstration hardware.

TABLE 2.—MACHINE PARAMETERS USED IN EXPERIMENTAL WORK

Machine Parameter	Value
J	4.65×10^{-4} kg-m^2
L_s	110 μH
R_s	0.06 Ω
λ_{af}	0.0144 volt-sec
Poles	4
Rated torque	1.5 N-m
Rated current	24 amps (rms)

The machine used in the experiment was available from a previous program and was used only to demonstrate the feasibility of the starting procedure on a PM machine. It was not intended to be completely representative of a potential JIMO alternator machine.

Dynamometer

The Magtrol dynamometer is a hysteresis brake. The load torque is produced by energizing a magnetic pole structure on the stationary portion of the dynamometer. This causes a magnetic field in the air gap that restrains the dynamometer rotor from spinning. The magnetic pole structure is energized with a field coil. The more current in the field coil, the larger the load torque produced. The amount of current in the field coil can be controlled from the Magtrol controller. A certain amount of current is provided to the field coil for each setting from 0 to 100 percent of total available load torque. The dynamometer can provide load torque at all speeds, including zero.

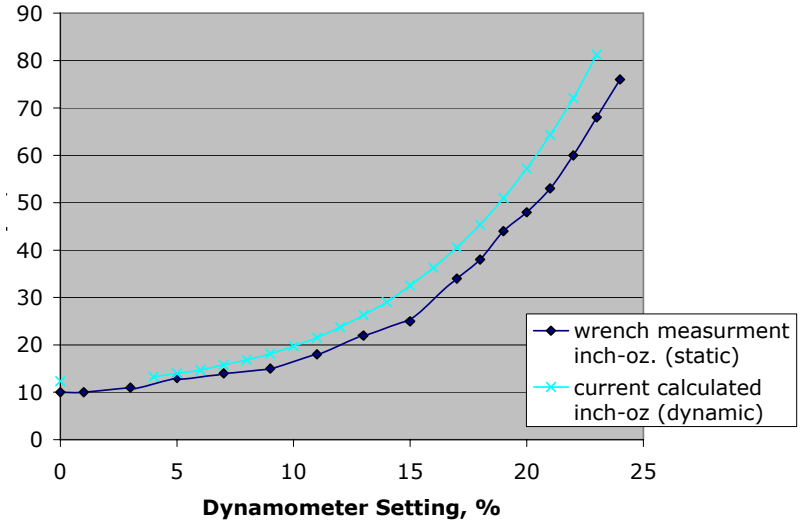

Figure 10.—Dynamometer load torque as a function of open loop setting.

The load torque as a function of percentage setting was measured statically and dynamically as follows. For the static measurement, a torque wrench was used. The percentage settings were gradually increased to a peak value of 24 percent and the torque measurement recorded. The results are shown in figure 10. For the dynamic measurement, the machine was held to a constant speed of 2000 rpm by the dSpace motor controller. Then the dynamometer percentage settings were increased and the peak current necessary to hold 2000 rpm for each value of setting was noted. The dynamometer torque can be computed from the peak current measurement by assuming perfect field orientation control and from knowledge of the back EMF constant according to equation (11) where λ_{af} is the back EMF constant, i^r_{qs} is the magnitude of the phase current and P is the number of poles of the machine.

$$\tau = \frac{3P}{4}\lambda_{af}\, i^r_{qs} \tag{11}$$

Both torque calibration results are shown in figure 10. It can be seen that at the higher levels of percentage settings the dynamic measurement indicates a higher torque value than the static measurements. The dynamic measurement is actually measuring the torque produced by the PM machine and assuming that it equals the torque produced by the dynamometer. In reality, the machine torque is equal to the dynamometer torque plus any mechanical losses in the system. The difference between the static measurements and the dynamic measurements shown in figure 10 is most likely due to these losses.

Experimental Results

An open loop start with a transition to field orientation and then to closed loop speed control was demonstrated for four values of constant load torque corresponding to the percentage load settings on the dynamometer of 0, 12, 18, and 23 percent, respectively. Based on the measurements reported in figure 10, this corresponds to approximately 0, 10, 20, and 30 percent of rated torque for this machine. The controller parameters remained the same for each load value. From t = 0 to ~30 seconds, the machine was accelerating using a ramped frequency command with a ramp rate of 10 rpm/second. When the speed reached 300 rpm, the control switched from the open loop ramp to the field orientation (vector) control. The machine then accelerated more quickly under field orientation because the current in the stator windings of the machine was optimally placed with respect to the rotor magnetic field. When the machine

reached 2,000 rpm, the speed loop was activated and the speed was regulated to the set point of 2,000 rpm. Once the speed loop was engaged, higher speeds could be achieved by changing the set point value. This is shown with a ramped speed command (100 rpm/sec) to 4,000 rpm for each case. The results are shown in figures 11 through 18.

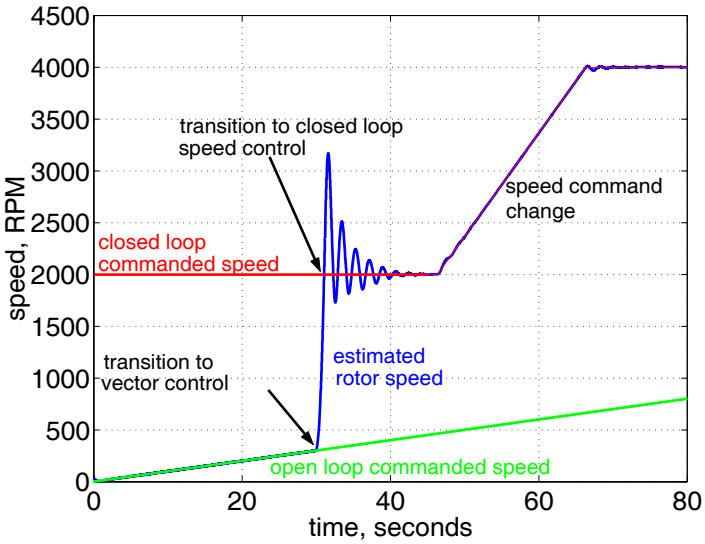

Figure 11.—Speed of PM machine using sensorless starting with no dynamometer load torque.

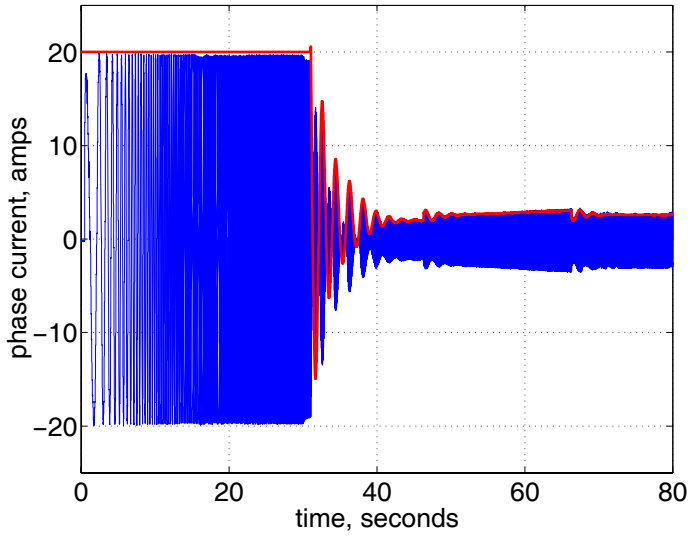

Figure 12.—Phase current of PM machine during start sequence with no dynamometer load torque.
(red: commanded magnitude, blue: measured)

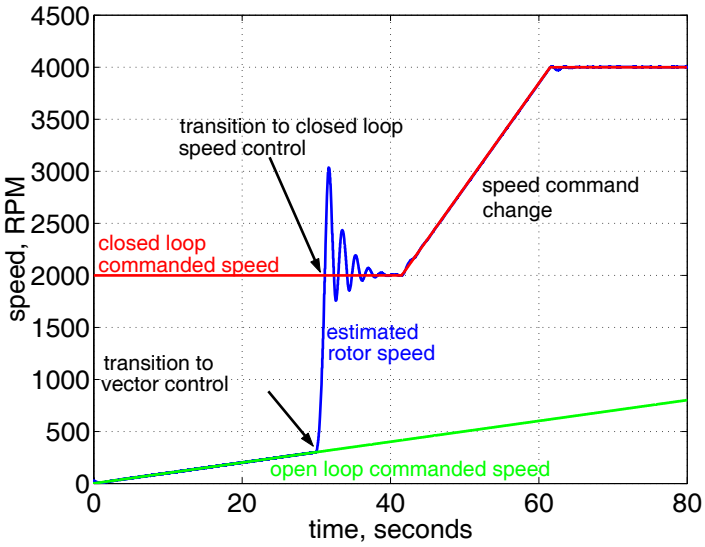

Figure 13.—Speed of PM machine using sensorless starting with ~10 percent of rated load torque.

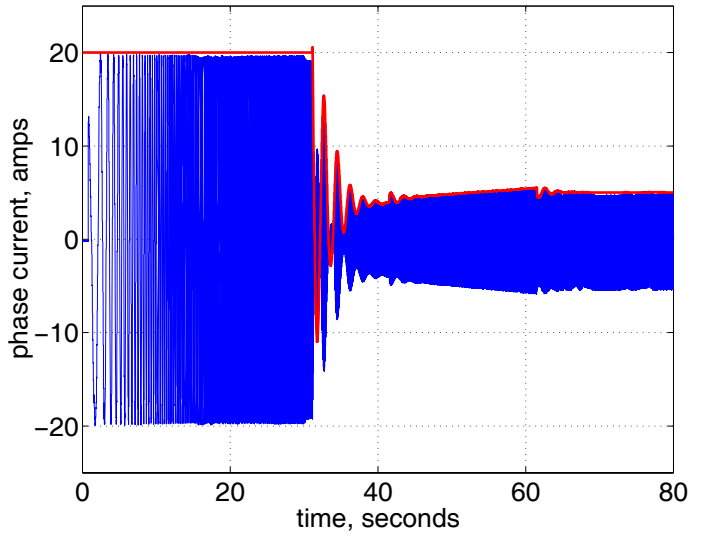

Figure 14.—Phase current of PM machine during start sequence with ~10 percent of rated load torque. (red: commanded magnitude, blue: measured)

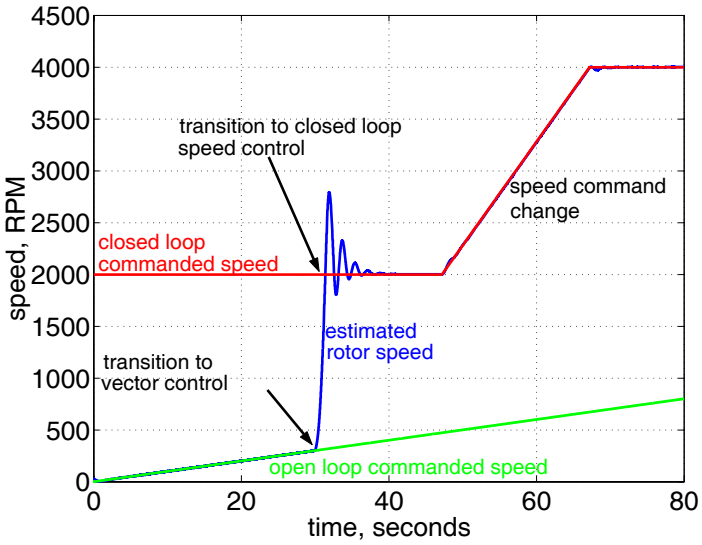

Figure 15.—Speed of PM machine using sensorless starting with ~20 percent of rated load torque.

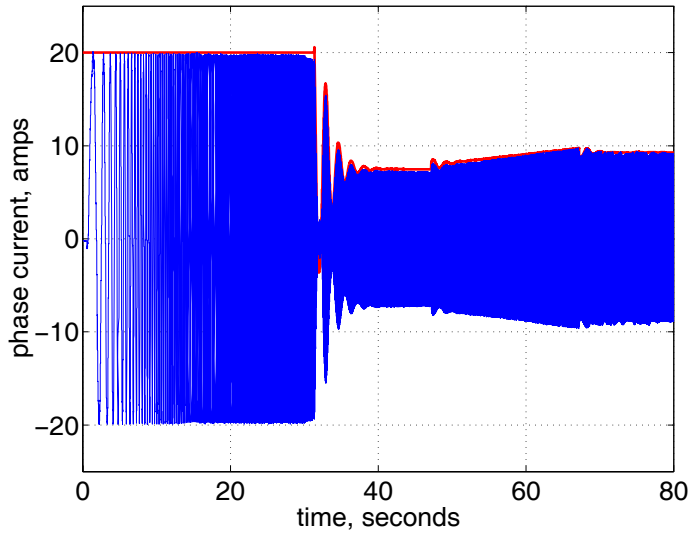

Figure 16.—Phase current of PM machine during start sequence with ~20 percent of rated load torque. (red: commanded magnitude, blue: measured)

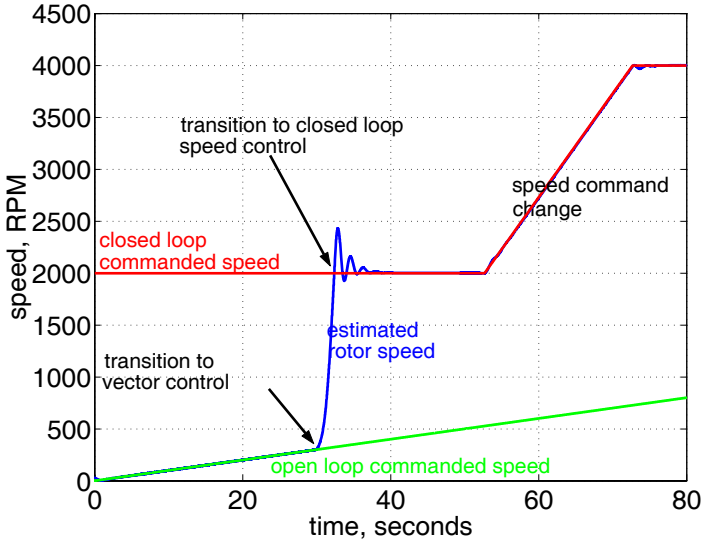

Figure 17.—Speed of PM machine using sensorless starting with ~30 percent of rated load torque.

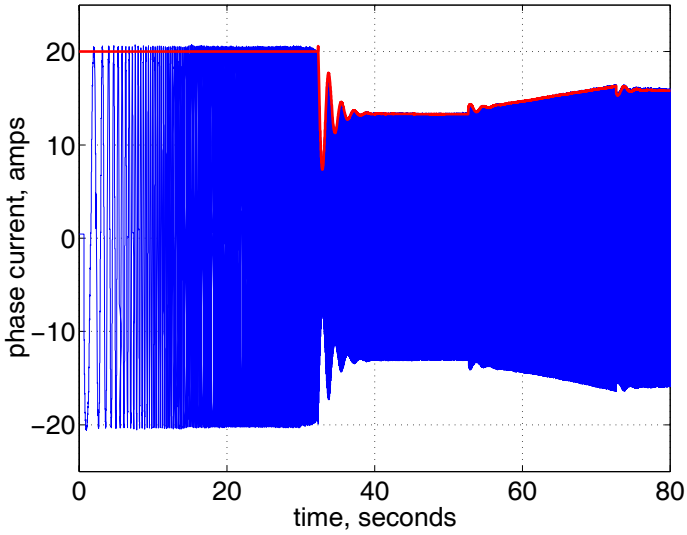

Figure 18.—Phase current of PM machine during start sequence with ~30 percent of rated load torque. (red: commanded magnitude, blue: measured)

The various controller gains were set with the maximum load torque applied (30% of rated). The gains included the current regulator gains, the speed observer gains (see fig. 4) and the speed regulator gains. In addition, the commanded values of the open loop ramp rate and the current value were selected. In general, setting the gains appropriately for any controller is a combination of experience, analysis and testing and this was no exception. A few remarks can be made here about the settings but when the final JIMO alternator hardware is designed and built, the controller will have to be appropriately tuned during testing.

The current regulator was tuned for a lower bandwidth than is typical for a field orientation application. Typically, a 1 to 2 kHz bandwidth is achievable for field orientation but during open loop starting, a fast response could cause the machine to lose synchronism as it was accelerating. So the

bandwidth was reduced to the 200 to 500 Hz range. The speed observer bandwidth must be fast enough to accommodate any necessary acceleration rates. This was particularly noticeable in simulation (where high acceleration rates were used) but experimentally a bandwidth of ~100 Hz worked well. Both the current regulator and the speed observer gains worked well for all values of load torques.

The other settings: open loop ramp rate, commanded current value and speed regulator gains, did make a difference on performance as the load torques were changed. In particular, for a lighter load torque, the ramp rate could be increased and the commanded current value could be decreased. For example, as the load was increased, the machine would not start in open loop with a commanded current value that was too low. Additionally, if the ramp rate was set too high for a particular load, the machine would lose synchronism as it started to accelerate. In general, heavier load torques required a slower ramp rate and a higher commanded current value than lighter load torques.

The speed oscillations seen in figures 11, 13, 15, and 17 occurred at the transition when the speed loop was closed (at 2000 rpm) and were heavily affected by the speed regulator gains. All of the gains were tuned for the 30 percent load case and then those gains were used for the other cases. The 30 percent loading was selected because that was similar to what has been observed experimentally with the 2 kW Brayton unit (ref. 1). For the 0 percent load case (fig. 11) the machine accelerates very quickly once field orientation (at $t \approx 30$ seconds) is achieved due to the high current command. The high acceleration rate of the machine in conjunction with the speed regulator gains causes it to overshoot the 2000 rpm set point when the speed loop is closed and then oscillate back to the commanded value. As the load is increased, the response improves (the magnitude of the oscillations decreases) because the system gains were set using the 30 percent load case.

It can be seen that the PM machine will start under all four conditions even though it was only tuned for the highest load torque case. This is an encouraging result because it shows that the foil bearing drag does not have to be predicted exactly in order to tune the controller to start the machine. The controller can be tuned for the expected bearing drag torque during testing but it is robust enough to operate with a different load torque. It also should be noted that the actual speed was not measured. The speed results shown on the plots are the estimated ones. In the future the actual speed should be measured to see if there is ringing in the speed during open loop starting as observed in the simulations.

Conclusions

A permanent magnet machine would be a likely candidate for the alternator for a JIMO-type mission. This machine could also operate as a motor during start up to begin to circulate the helium-xenon gas of the Brayton cycle. This work has shown in simulation and experimentally that position- and speed-sensorless starting of a permanent magnet machine under varying load torques is feasible. Experimentally it was shown that the machine could start with one set of gains in the controller over a range of load torques from 0 to 30 percent of rated. This is important because it demonstrates the robustness of the control in the presence of significant load variations.

In the future, more tests should be conducted with a load torque profile during start up that mimics the drag that would expected due to the foil bearings. Additionally, the speed should be measured and compared to the estimated value. Finally, the controller should be applied to the demonstration 2 kW Brayton unit that has a PM alternator and foil bearings to demonstrate the feasibility on a more realistic experimental model.

References

1. Hervol, David, Mason, Lee, Birchenough, Art, and Pinero, Luis; “Experimental Investigations from the Operation of a 2 kW Brayton Power Conversion Unit and Xenon Ion Thruster,” NASA TM—2004-212960, *Proceedings of the Space Technology and Applications International Forum (STAIF-2004),* Albuquerque, NM, Feb. 8–12, 2004.

2. Vas, Peter; *Sensorless Vector and Direct Torque Control*, Oxford University Press, New York, NY, 1998.
3. Patel, N., T. O'Meara, J. Nagashima, and R. Lorenz, "Encoderless IPM Traction Drive for EV/HEV's," *Conference Record of the 2001 IEEE Industry Applications Conference*, Chicago, IL.
4. Wu, Rusong and Slemon, Gordon; "A Permanent Magnet Motor Drive Without a Shaft Sensor," *IEEE Transactions on Industry Applications*, Vol. 27, No. 5, September/October 1991, pp. 1005–1011.
5. Matsui, Nobuyuki; "Sensorless PM Brushless DC Motor Drives," *IEEE Transactions on Industrial Electronics*, Vol. 43, No. 2, April, 1996, pp. 300–308.
6. Jansen, Patrick and Robert D. Lorenz, "Transducerless Position and Velocity Estimation in Induction and Salient AC Machines," *IEEE Transactions on Industry Applications*, Vol. 31, No. 2, March/April 1995 pp. 240–247.
7. Schroedl M., "Sensorless control of AC machines at low speed and standstill based on the "INFORM" method," *Conference Record of the Thirty-First IEEE Industry Applications Society Annual Meeting*, October 6–10, 1996, Vol. 1, pp. 270–277.
8. Krishnan, Ramu, *Permanent Magnet Synchronous and Brushless DC Motor Drives: Theory, Operation, Performance, Modeling, Simulation, Analysis and Design*, Virginia Tech., Blacksburg, Virginia, 1999.
9. Krause, Paul, *Analysis of Electric Machinery*, McGraw-Hill Book Company, New York, New York, NY, 1986.
10. Novotny, Donald; Lipo, Thomas; *Vector Control and Dynamics of AC Drives,* Oxford University Press, New York, NY, 1996.
11. Mohan, Ned; *Advanced Electric Drives*, MNPERE, Minneapolis, MN, 2001.
12. Rowan, T. and R. Kerkman, "A New Synchronous Current Regulator and an Analysis of Current-Regulated PWM Inverters," *IEEE Transactions on Industry Applications*, Vol. IA-22, No. 4, July/August 1986, pp. 678–690.
13. Holtz, Joachim, "Pulsewidth Modulation for Electronic Power Conversion*," Proceedings of the IEEE*, Vol. 82, No. 8, August, 1994, pp. 1194–1214.
14. DellaCorte, C.; Lukaszewicz, V.; Valco, M.J.; Radil, K.C.; Heshmat, H.; "Performance and Durability of High Temperature Foil Air Bearings for Oil-Free Turbomachinery," NASA/TM—2000-209187/Rev. 1, *Proceedings of the Society of Tribologists and Lubrication Engineers Annual Meeting, Nashville*, TN., May 7–11, 2000.
15. Lorenz, Robert D., K.W. Van Patten, "High-resolution velocity estimation for all-digital, AC servo drives" *IEEE Transactions on Industry Applications*, Vol. 27, No. 4, July/August 1991, pp. 701–705.

REPORT DOCUMENTATION PAGE

Form Approved
OMB No. 0704-0188

1. AGENCY USE ONLY (*Leave blank*)	2. REPORT DATE	3. REPORT TYPE AND DATES COVERED
	February 2006	Technical Memorandum

4. TITLE AND SUBTITLE

Feasibility Study of Jupiter Icy Moons Orbiter Permanent Magnet Alternator Start Sequence

5. FUNDING NUMBERS

WBS–22–982–10–50

6. AUTHOR(S)

Barbara H. Kenny and Roger P. Tokars

7. PERFORMING ORGANIZATION NAME(S) AND ADDRESS(ES)

National Aeronautics and Space Administration
John H. Glenn Research Center at Lewis Field
Cleveland, Ohio 44135–3191

8. PERFORMING ORGANIZATION REPORT NUMBER

E–15391

9. SPONSORING/MONITORING AGENCY NAME(S) AND ADDRESS(ES)

National Aeronautics and Space Administration
Washington, DC 20546–0001

10. SPONSORING/MONITORING AGENCY REPORT NUMBER

NASA TM—2006-214034

11. SUPPLEMENTARY NOTES

Barbara H. Kenny, e-mail: Barbara.H.Kenny@nasa.gov, NASA Glenn Research Center; and Roger P. Tokars, e-mail: RTokars@purdue.edu, Purdue University, Electrical and Computer Engineering Department, 1 Purdue University, West Lafayette, Indiana 47907. Responsible person, Barbara H. Kenny, organization code RPE, 216–433–6289.

12a. DISTRIBUTION/AVAILABILITY STATEMENT

Unclassified - Unlimited
Subject Categories: 44 and 20

Available electronically at http://gltrs.grc.nasa.gov

This publication is available from the NASA Center for AeroSpace Information, 301–621–0390.

12b. DISTRIBUTION CODE

13. ABSTRACT ***(Maximum 200 words)***

The Jupiter Icy Moons Orbiter (JIMO) mission was a proposed, (recently cancelled) long duration science mission to study three moons of Jupiter: Callisto, Ganymede, and Europa. One design of the JIMO spacecraft used a nuclear heat source in conjunction with a Brayton rotating machine to generate electrical power for the electric thrusters and the spacecraft bus. The basic operation of the closed cycle Brayton system was as follows. The working fluid, a helium-xenon gas mixture, first entered a compressor, then went through a recuperator and hot-side heat exchanger, then expanded across a turbine that drove an alternator, then entered the cold-side of the recuperator and heat exchanger and finally returned to the compressor. The spacecraft was to be launched with the Brayton system off-line and the nuclear reactor shut down. Once the system was started, the helium-xenon gas would be circulated into the heat exchangers as the nuclear reactors were activated. Initially, the alternator unit would operate as a motor so as to drive the turbine and compressor to get the cycle started. This report investigated the feasibility of the start up sequence of a permanent magnet (PM) machine, similar in operation to the alternator unit, without any position or speed feedback sensors ("sensorless") and with a variable load torque. It is found that the permanent magnet machine can start with sensorless control and a load torque of up to 30 percent of the rated value.

14. SUBJECT TERMS

Permanent magnet machine; Sensorless control; Alternator; Sensorless starting

15. NUMBER OF PAGES

23

16. PRICE CODE

17. SECURITY CLASSIFICATION OF REPORT	18. SECURITY CLASSIFICATION OF THIS PAGE	19. SECURITY CLASSIFICATION OF ABSTRACT	20. LIMITATION OF ABSTRACT
Unclassified	Unclassified	Unclassified	